

## Experimental lifetime of the $a^1\Delta$ electronically excited state of $\text{CH}^-$

Gustav Eklund<sup>1,\*</sup>, Moa K. Kristiansson<sup>1</sup>, K. C. Chartkunchand<sup>2</sup>, Emma K. Anderson<sup>3</sup>, Malcolm Simpson<sup>4</sup>, Roland Wester<sup>4</sup>, Henning T. Schmidt<sup>1,†</sup>, Henning Zettergren<sup>1</sup>, Henrik Cederquist<sup>1</sup>, and Wolf D. Geppert<sup>1</sup>

<sup>1</sup>Department of Physics, Stockholm University, Stockholm 10691, Sweden

<sup>2</sup>Atomic, Molecular and Optical Physics Laboratory, RIKEN, Saitama 351-0198, Japan

<sup>3</sup>Department of Physics and Astronomy, Aarhus University, 8000 Aarhus C, Denmark

<sup>4</sup>Institut für Ionenphysik und Angewandte Physik, Universität Innsbruck, Technikerstraße 25, 6020 Innsbruck, Austria



(Received 1 November 2021; accepted 24 December 2021; published 11 February 2022)

By repeatedly probing the  $a^1\Delta$  excited state and the  $X^3\Sigma^-$  ground-state populations in a beam of  $\text{CH}^-$  ions stored in a cryogenic ion-beam storage ring for 100 s, we extract an intrinsic lifetime of  $14.9 \pm 0.5$  s for this excited state. This is far longer than all earlier experimental and theoretical results, exposing large difficulties in measuring and calculating slow decays and the need for benchmark quality experiments.

DOI: [10.1103/PhysRevResearch.4.L012016](https://doi.org/10.1103/PhysRevResearch.4.L012016)

Molecular anions play important roles in the interstellar medium and planetary ionospheres. Around a decade ago, hydrocarbon and cyano anions ( $\text{CN}^-$ ,  $\text{C}_3\text{N}^-$ ,  $\text{C}_4\text{H}^-$ ,  $\text{C}_5\text{N}^-$ ,  $\text{C}_6\text{H}^-$ , and  $\text{C}_8\text{H}^-$ ) were observed in circumstellar envelopes and dark interstellar clouds [1]. Discoveries of  $\text{C}_6\text{H}^-$  in several star forming regions [2] revealed that anions are widespread in the interstellar medium and not restricted to environments with unusual physical or chemical conditions. The Plasma Spectrometer on board the CASSINI spacecraft has led to the discovery of a multitude of anions in the ionosphere of Saturn's moon Titan, where the strongest anion signals were recorded at a mass-to-charge ratio of  $m/z = 1000$  u [3]. However, the nature of these large negative ions remains unclear. On the other hand, the smaller ions  $\text{CN}^-$ ,  $\text{C}_3\text{N}^-$ , and  $\text{C}_5\text{N}^-$  have been identified by the CASSINI mission. Furthermore, a recent calculation has shown that  $\text{CH}^-$  may be efficiently produced in reactions between  $\text{CH}_2$  and  $\text{H}^-$ , which may be of importance for the understanding of Titan's and Saturn's [4] atmospheres and for planetary atmospheres more generally.

Previous experimental and theoretical studies of the  $\text{CH}^-$  molecular ion has focused mainly on the electronic structure. In an early study, Feldmann [5] applied near-threshold photodetachment spectroscopy, and observed two distinct thresholds in the photodetachment spectrum, from which a value of  $0.74 \pm 0.05$  eV for the electron affinity of CH was deduced [5]. This low value was not reproduced in later photoelectron spectroscopy experiments by Kasdan *et al.* [6] or Goebbert [7], who measured  $1.238 \pm 0.008$  eV and  $1.26 \pm$

$0.02$  eV, respectively. Calculations of the electron affinity are mostly consistent with the more recent experimental results, ranging 1.0–1.9 eV (see, e.g., Ref. [8]).

The molecular anion  $\text{CH}^-$  has an electronically excited state with  $^1\Delta$  symmetry (see Fig. 1). This state was identified in the experiment by Kasdan *et al.* at an energy of  $0.845 \pm 0.012$  eV above the ground state [6]. This  $a^1\Delta$  state is expected to be long lived, as the radiative transition to the  $X^3\Sigma^-$  ground state is forbidden by spin selection rules. Okumura *et al.* [9] have performed the only earlier measurement of the  $a^1\Delta$  lifetime. In their experiment, they stored  $\text{CH}^-$  ions in a radio-frequency ion trap at room temperature for up to about 5 s. A laser operating at 1.16 eV was used to photodetach the  $a^1\Delta$  state. For each ion-bunch injection, a single laser pulse was fired. After the pulse, the trap was emptied and the remaining ions were detected. By repeating the measurement as a function of the time of firing the laser pulse, and comparing the number of remaining ions with and without the laser pulse, the fraction of photodetached ions was determined and an  $a^1\Delta$  lifetime of  $5.9 \pm 0.8$  s was deduced [9]. An additional fast decay with a lifetime of  $1.75 \pm 0.15$  ms was also observed by Okumura *et al.* [9], and assigned to the first excited vibrational state of the  $X^3\Sigma^-$  electronic ground state. Furthermore, lower and upper bounds on the electron affinity of 1.16 and 1.68 eV were deduced in the same experiment [9]. Theoretical calculations of the  $a^1\Delta$  lifetime are very challenging as the radiative transition relies on mixing with electronic continuum states through spin-orbit coupling. This phenomenon was studied by Lengsfeld *et al.* [10], who calculated  $6.14 \pm 1.2$  s in agreement with the experiment by Okumura *et al.* [9]. A later theoretical study by Srivastava *et al.* [11] yielded a value of 5.63 s, in agreement with all experimental [9] and theoretical results [10] available at the time. This seemed to indicate a good understanding of the decay of the  $a^1\Delta$  state in  $\text{CH}^-$  and thus of slow molecular decay processes in general.

In the present study, we measure the radiative lifetime of the  $a^1\Delta$  state using a beam of  $\text{CH}^-$  stored for up to 100 s in

\*gustav eklund@fysik.su.se

†schmidt@fysik.su.se

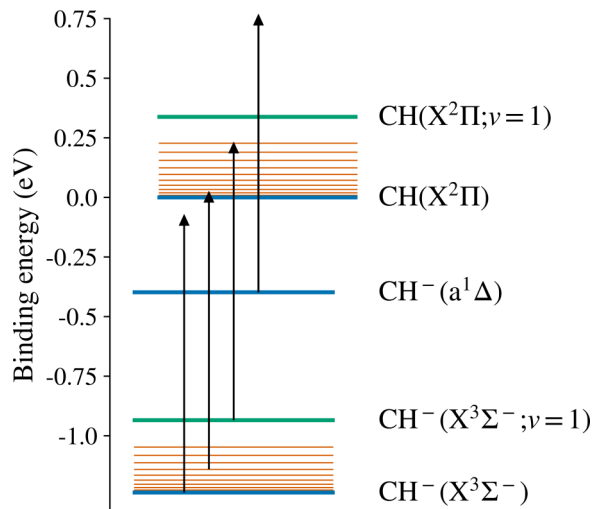


FIG. 1. Schematic energy level diagram of the electronic structure of CH and CH<sup>-</sup>. For the electronic ground states, the first vibrational and rotational excited states are also indicated by the green and orange lines, respectively. The photon energy of 1.16 eV used in the present experiment and by Okumura *et al.* [9] is represented by the vertical arrows.

one of the cryogenic ion-beam storage rings of the DESIREE facility [12,13]. This allows the ions to decay to the vibrational ground state and relax their rotational excitations [14]. The lifetime is measured by repeatedly probing the stored ion beam through photodetachment by laser pulses [15–17]. DESIREE consists of two electrostatic ion-beam storage rings with a common straight section for merged-beams studies of sub-eV ion-ion collisions [12,13]. The storage rings are enclosed in a single vacuum chamber and cryogenically cooled to a temperature of  $13.5 \pm 0.5$  K. Beams of CH<sup>-</sup> are produced in a cesium-sputter ion source, using ethanol vapor. Typically, a large fraction of ions produced from such a source are hot, and occupy a large number of excited vibrational and rotational states of the ground state and of the electronically excited metastable state of interest. The CH<sup>-</sup> ions are extracted from the source and accelerated to 10 keV, and are mass selected using a bending magnet. The ion beam is then transported and injected into the storage ring as shown in Fig. 2. Typical CH<sup>-</sup> currents are about 4 nA. After injection, the ion beam is stored for 100 s, after which it is extracted from the ring and dumped into a Faraday cup to measure the remaining ion current. The light used for photodetachment is provided by a pulsed optical parametric oscillator (OPO), arranged to interact with the ion beam in a perpendicular configuration in one of the straight sections of the ring (see Fig. 2). The OPO has a repetition rate of 10 Hz, and the photon energy is widely tunable (with a linewidth of 6 meV), but set to 1.160 eV for the present experiment.

When photodetachment occurs, the resulting neutral CH molecules are no longer confined by the electrostatic elements of the storage ring, and continue along their straight-line trajectories to an imaging detector. This detector consists of a triple stack of microchannel plates (MCPs) and a phosphor screen [18]. The light from the phosphor screen is detected by a photomultiplier tube. Since the time of flight for

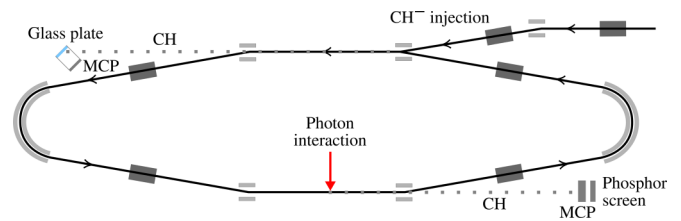


FIG. 2. Schematic of the storage ring used in the experiment. A pulsed (10 Hz) OPO beam, tuned to 1.160 eV, is used for photodetachment in a perpendicular orientation, and the resulting neutral products are detected using a microchannel plate (MCP) stack, a phosphor screen, and a photomultiplier tube (not shown). Following the other straight section of the ring, neutral CH molecules are detected by a system consisting of a metal-coated glass plate for secondary electron emission, an MCP stack, and a resistive anode.

the neutrals from the photon interaction region to the detector is known, the influence of detector background is considerably decreased by making use of the temporal coincidence between the laser pulse and the arrival of the neutral products at the detector. Following the other straight section of the ring, another detector is mounted. This second detector system contains as its front element a titanium- and gold-coated glass plate. As neutral particles hit the glass plate, secondary electrons are emitted and detected by an MCP detector. This second detector system is used to monitor the decay of the ion beam. At the present photon energy of 1.160 eV, photodetachment from vibrationally excited states of the  $X^3\Sigma^-$  ground state is possible, as indicated in Fig. 1. However, the lifetimes of these states are on the order of milliseconds [9,19], and their contribution is negligible on the much longer timescales expected for the decay of the  $a^1\Delta$  state [9–11]. Photodetachment from very highly excited rotational states of the  $X^3\Sigma^-$  state is energetically possible as well (see Fig. 1). High rotational states are known to be populated in sputter ion sources, which has been seen in experiments on long timescales by infrared inactive metal dimer anions [20,21]. However, photodetachment from such states is unlikely in the present experiment on CH<sup>-</sup> as energy conservation would require large changes of rotational quantum numbers. This would violate the selection rules for electric dipole transitions between rotational states. Thus, we assume that only the  $a^1\Delta$  state is contributing to the photodetachment signal at the present photon energy.

The ion beam is continuously probed using the OPO throughout the full 100 s of each individual storage cycle. The resulting photodetachment rate  $P(t)$  is shown by the black data points in the top panel of Fig. 3. The data are collected over 476 separate 100-s ion storage cycles, and a histogram is constructed with a bin width of 2 s. The observed number of events are assumed to follow Poisson statistics, and the uncertainty is taken as the square root of the number of events in each bin. To deduce the rate  $P(t)$ , the data are divided by the number of ion storage cycles and by the 2-s bin width. A characteristic exponential decay is clearly observed, with a far longer lifetime of the  $a^1\Delta$  state than the previously measured value of  $5.9 \pm 0.8$  s [9] and the earlier calculated values of  $6.14 \pm 1.2$  s and 5.63 s, respectively [10,11].

In order to investigate if an excited state of  $^{13}\text{C}^-$  ( $1s^2 2s^2 2p^3 \ ^2\text{D}$ ) could be present in the circulating  $^{12}\text{CH}^-$

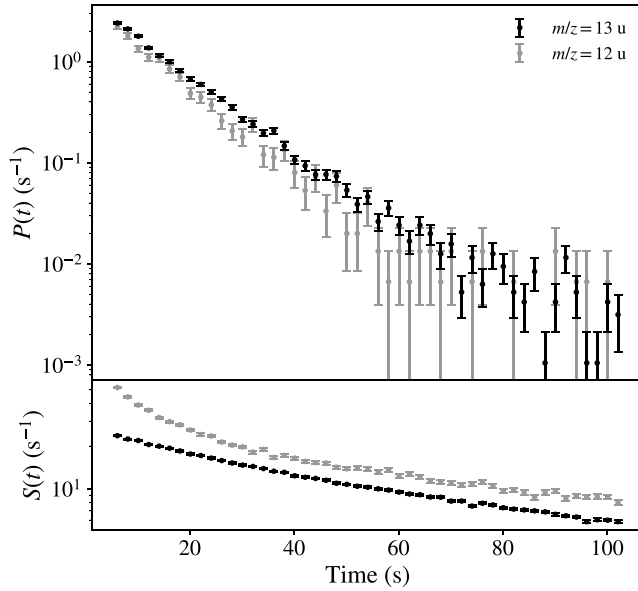


FIG. 3. Detected rate for  $m/z = 13$  u (black data) and  $m/z = 12$  u (grey data). The measurement at  $m/z = 12$  u is performed to probe a possible  $^{13}\text{C}^-$  contamination of the  $\text{CH}^-$  beam (see main text). Top: Measured photodetachment yield on the imaging detector,  $P(t)$ , as a function of time at a photon energy of 1.160 eV. Bottom: Yield on the glass plate detector system,  $S(t)$ . The rapid decay in the grey data is possibly related to the excited  $1s^2 2s^2 2p^3 \ ^2\text{D}$  state of  $\text{C}^-$ .

beam and influence the present result, we performed additional measurements for a separately stored  $^{12}\text{C}^-$  beam. The bending magnet was then set to select ions with  $m/z = 12$  u, while leaving all other experimental conditions the same as for the  $m/z = 13$  u beam. The  $m/z = 12$  u data were recorded over 75 ion storage cycles, and analyzed in the same way as the  $m/z = 13$  u measurement. The resulting  $P(t)$  for  $m/z = 12$  u is shown by the grey data in the upper panel of Fig. 3. The observed decay appears similar to the decay at  $m/z = 13$  u. However, note that the two measurements of  $P(t)$  in the top panel of Fig. 3 are nearly identical in magnitude. Recorded mass spectra during the experiment indicated that the ion currents for  $m/z = 12$  u and  $m/z = 13$  u were comparable. Furthermore, the average ion current recorded in the Faraday cup where the beam is ejected was about 3.82 and 3.75 nA for  $m/z = 12$  u and  $m/z = 13$  u, respectively. With the present experimental conditions, these measured currents imply that the number of stored ions in the  $m/z = 13$  u beam was about 6% larger than the number of stored ions in the  $m/z = 12$  u beam. As the natural abundance of  $^{13}\text{C}$  is about 1.1% [22], the estimated ratio of the number of stored ions in the two beams would indicate that about 1% of the ion beam at  $m/z = 13$  u consists of  $^{13}\text{C}^-$ , while 99% is  $^{12}\text{CH}^-$ . Thus, the fact that the rates for the two measurements of  $P(t)$  are similar indicates that the signal at  $m/z = 13$  u is almost completely dominated by the  $\text{CH}^-$  contribution. Any  $^{13}\text{C}^-$  contribution to  $P(t)$  at  $m/z = 13$  u must be one hundred times smaller than  $P(t)$  at  $m/z = 12$  u.

In the bottom panel of Fig. 3, the measured rates of neutral particles as observed on the detector at the other straight section of the ring  $S(t)$  are shown. For both beams  $S(t)$  is

analyzed analogously to  $P(t)$ , but the detector dark count rate is subtracted [the detector background is negligible for  $P(t)$  due to the temporal coincidence setup]. The rates  $P(t)$  and  $S(t)$  in Fig. 3 are thus directly comparable. The rate  $S(t)$  observed for  $m/z = 12$  u (grey data) shows a distinct decay during the first 40 s of storage, whereas the data  $m/z = 13$  u show no, or a very weak, indication of such a decay. The timescale of this decay is very similar to the decay observed in  $P(t)$  for  $m/z = 12$  u, and it is likely due to the excited  $1s^2 2s^2 2p^3 \ ^2\text{D}$  state of  $\text{C}^-$ . This state has a binding energy of 33 meV, and a predicted radiative lifetime on the order of  $10^5$  s [23]. However, since the state is loosely bound, the electron may be detached by black-body radiation, in collisions with residual gas, or through some other mechanism. The absence of this decay in the data recorded at  $m/z = 13$  u is consistent with the conclusion above that the contamination of  $^{13}\text{C}^-$  in the  $^{12}\text{CH}^-$  beam is insignificant. Thus the  $P(t)$  and  $S(t)$  data recorded with the  $\text{CH}^-$  beam can be directly used to deduce the inherent lifetime of the  $a^1\Delta$  state in  $\text{CH}^-$  as described in the following.

In order to extract the lifetime of the  $a^1\Delta$  state from the data in Fig. 3, we treat  $\text{CH}^-$  as a two-level system consisting of the  $X^3\Sigma^-$  ground state and the excited  $a^1\Delta$  state. Let  $N_\Sigma$  and  $N_\Delta$  be the number of ions in the respective state, and let  $\dot{N}_\Sigma$  and  $\dot{N}_\Delta$  be the corresponding derivatives with respect to time. The time evolution of the populations of the two states is governed by a system of differential equations,

$$\begin{aligned}\dot{N}_\Delta &= -(\Gamma_\Delta + k_\Delta + k_{\text{pd}})N_\Delta \\ \dot{N}_\Sigma &= -k_\Sigma N_\Sigma + \Gamma_\Delta N_\Delta,\end{aligned}\quad (1)$$

where  $\Gamma_\Delta$  is the decay constant for the  $a^1\Delta$  state,  $k_\Sigma$  and  $k_\Delta$  are the losses of ions from the beam due to collisions with residual gas or intrabeam scattering, and  $k_{\text{pd}}$  is the loss rate due to photodetachment. Note that Eqs. (1) do not contain any mechanisms for excitation or deexcitation. The rates for such processes are expected to be small in comparison to collisional detachment processes due to the low final state densities. Furthermore, collisional detachment is not the main contribution to  $k_\Sigma$  and  $k_\Delta$  as we shall see below. Assuming the beam losses are independent of the electronic state  $k_\Sigma = k_\Delta = k$ , and also that they are the dominating losses, such that  $k_{\text{pd}} \ll k$ , Eqs. (1) reduce to

$$\begin{aligned}\dot{N}_\Delta &= -\Gamma_\Delta N_\Delta - k N_\Delta \\ \dot{N}_\Sigma &= -k N_\Sigma + \Gamma_\Delta N_\Delta.\end{aligned}\quad (2)$$

The solutions are

$$\begin{aligned}N_\Delta(t) &= C_1 e^{-(k+\Gamma_\Delta)t} \\ N_\Sigma(t) &= C_2 e^{-kt} - C_1 e^{-(k+\Gamma_\Delta)t},\end{aligned}\quad (3)$$

where  $C_1$  and  $C_2$  are constants. Under the assumption leading to the solution in Eqs. (3), the photodetachment signal  $P(t)$  in Fig. 3 is  $P(t) = k_{\text{pd}} N_\Delta$ , and  $S(t)$  in Fig. 3 is  $S(t) = k(N_\Sigma + N_\Delta)$ . The ratio is then

$$\frac{P(t)}{S(t)} \propto e^{-\Gamma_\Delta t}.\quad (4)$$

Thus, this ratio depends only on  $\Gamma_\Delta$ . The  $P(t)/S(t)$  data are shown in Fig. 4 and yield a preliminary value of  $1/\Gamma_\Delta$  of

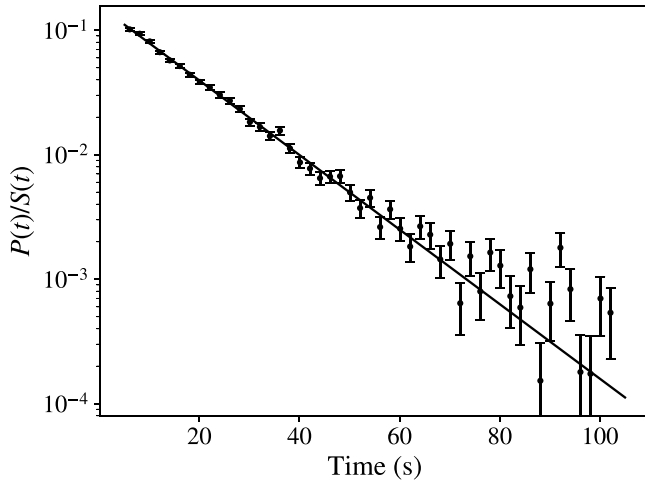


FIG. 4. The ratio of the measured photodetachment rate with the OPO,  $P(t)$  to the beam-loss rate,  $S(t)$ , as a function of storage time  $t$ . The ratio  $P(t)/S(t)$  is proportional to the excited-state population fraction and reflects the decay of the  $a^1\Delta$  state of  $\text{CH}^-$ . A single exponential function is fitted to the data, from which the radiative lifetime is extracted as described in the text.

$14.5 \pm 0.2$  s. The validity of Eq. (4) is dependent on the approximations made in Eqs. (2). By comparing the value of  $P(t)$  at 100 s in Fig. 3, which is  $10^{-2} \text{ s}^{-1}$ , to the number of ions recorded when the ion beam is dumped (about  $5 \times 10^5$ ), and assuming a very low relative population in the  $a^1\Delta$  state of  $10^{-3}$  (about 500 ions), we arrive at  $k_{\text{pd}} = P(t = 100 \text{ s})/N_{\Delta}(t = 100 \text{ s}) = 2 \times 10^{-5} \text{ s}^{-1}$ . This is negligible compared to  $\Gamma_{\Delta} \approx 0.07 \text{ s}^{-1}$ . With a higher assumed relative population the estimate of  $k_{\text{pd}}$  becomes even smaller. The assumption that  $k_{\Sigma} = k_{\Delta}$  is somewhat more challenging to argue for, but on the other hand even rather drastic assumptions about differences between the rates have little influence on the final result. It is not possible to measure these rates separately in the present experiment and, while they are always small compared to  $\Gamma_{\Delta}$ , these two decay rates are varying in time due to a dependence on the ion-beam intensity [13]. The measurement of  $S(t)$  in the lower panel of Fig. 3 indicates a storage lifetime of about 100 s, whereas a separate long-time storage measurement yields  $300 \pm 50$  s (see Appendix B). This implies that during the first 100 s, where the  $a^1\Delta$  state decay takes place, other beam loss mechanisms besides collisions with the residual gas, e.g., intrabeam scattering, are important. The ratio  $P(t)/S(t)$ , shown in Fig. 4, is proportional to the relative population of the  $a^1\Delta$  state in the stored  $\text{CH}^-$  beam at all times  $t$ . Therefore, Eq. (4) may be used to deduce a good first estimate of  $\Gamma_{\Delta}$  regardless of the exact nature of the beam-loss mechanisms as long as these mechanisms are not too different for the  $a^1\Delta$  and  $X^3\Sigma^-$  states. Losses due to intrabeam scattering are caused by long-range Coulomb interactions between ions and should be independent of the quantum states, while the cross sections for detachment in collisions with  $\text{H}_2$ , which is the dominant component in the residual gas in DESIREE [13], may differ somewhat for the two states. However, the fact that  $S(t)$ —the black data in the lower panel of Fig. 3—is a single exponential function would be consistent with these two cross sections being

similar. A detailed analysis shows that the somewhat arbitrary assumption that the collisional detachment cross section for the  $a^1\Delta$  state falls in the range of that of the ground state and twice that value would give a systematic shift of  $0.4 \pm 0.4$  s in relation to a lifetime deduced directly from Eq. (4) (see Appendix C). In the final result for the  $a^1\Delta$  state lifetime we add this shift, resulting in a lifetime of  $14.9 \pm 0.5$  s.

Our result for the lifetime of the  $a^1\Delta$  state in  $\text{CH}^-$  of  $14.9 \pm 0.5$  s is a factor of about 2.5 longer than, and more than ten standard deviations from, that of Okumura *et al.* [9]. The main differences in the experimental conditions are the temperatures and pressures, which are very much lower in our case. Since the  $P(t)/S(t)$  data are described by a single exponential function with high precision as indicated by the comparison with the line in Fig. 4, it is highly unlikely that rotationally excited states with different lifetimes play a significant role here, while such influences would be more likely in room-temperature experiments [9]. Reliable absolute decay rates of electronically excited molecular anions will be crucial for correct estimates of abundances of such ions in planetary atmospheres and other astrophysical environments. Our experiment shows that the ability to store the ions at cryogenic temperature for much longer times than the lifetime to be measured is key for obtaining accurate and precise experimental results. In turn, such results are important to guide difficult and highly challenging theoretical calculations of the corresponding decay processes and thus for developing a more complete understanding of the properties of molecular anions in general.

This work was performed at the Swedish National Infrastructure, DESIREE (Swedish Research Council Contract No. 2017-00621) and is a part of the project “Probing charge- and mass-transfer reactions on the atomic level,” supported by the Knut and Alice Wallenberg Foundation (Grant No. 2018.0028). Furthermore, H.C., H.Z., H.T.S., and W.D.G. thank the Swedish Research Council for individual project grants (with Contracts No. 2019-04379, No. 2020-03437, No. 2018-04092, and No. 2019-04332). This Letter is based upon work from COST Action CA18212 - Molecular Dynamics in the GAS phase (MD-GAS), supported by COST (European Cooperation in Science and Technology). M.S. acknowledges support by the Austrian Science Fund FWF within the DK-ALM (Grant No. W1259-N27).

#### APPENDIX A: DERIVATION OF $P(t)/S(t)$

Writing Eq. (1) in matrix form we get

$$\begin{pmatrix} \dot{N}_{\Delta} \\ \dot{N}_{\Sigma} \end{pmatrix} = \begin{pmatrix} -(\Gamma_{\Delta} + k_{\Delta} + k_{\text{pd}}) & 0 \\ \Gamma_{\Delta} & -k_{\Sigma} \end{pmatrix} \begin{pmatrix} N_{\Delta} \\ N_{\Sigma} \end{pmatrix}. \quad (\text{A1})$$

The above matrix has the eigenvalues  $\lambda_1 = -k_{\Sigma}$  and  $\lambda_2 = -(\Gamma_{\Delta} + k_{\text{pd}} + k_{\Delta})$ . A set of corresponding eigenvectors are  $\vec{v}_1 = (0, 1)$  and  $\vec{v}_2 = (-\Gamma_{\Delta}, \Gamma_{\Delta} + k_{\text{pd}} + k_{\Delta} - k_{\Sigma})$ . The solutions to Eqs. (1) are then

$$\begin{pmatrix} N_{\Delta} \\ N_{\Sigma} \end{pmatrix} = C_1 e^{-k_{\Sigma} t} \begin{pmatrix} 0 \\ 1 \end{pmatrix} + C_2 e^{-(\Gamma_{\Delta} + k_{\text{pd}} + k_{\Delta}) t} \times \begin{pmatrix} -\Gamma_{\Delta} \\ \Gamma_{\Delta} + k_{\text{pd}} + k_{\Delta} - k_{\Sigma} \end{pmatrix}. \quad (\text{A2})$$

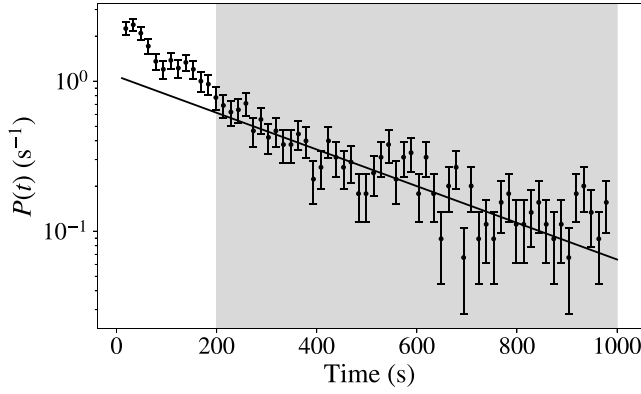


FIG. 5. Measured photodetachment rate  $P(t)$  at a photon energy of 1.240 eV. The observed decay is proportional to the number of ions in the beam. A typical fit with an exponential function is shown, where the grey area indicates the subset of the data included in the fit.

By introducing the initial conditions  $N_{\Sigma}(0) = N'_{\Sigma}$  and  $N_{\Delta}(0) = N'_{\Delta}$ , where  $N'_{\Sigma}$  and  $N'_{\Delta}$  are the initial populations of the  $X^3\Sigma^-$  state and  $a^1\Delta$  state respectively, the constants  $C_1$  and  $C_2$  are determined and Eqs. (A2) become

$$\begin{aligned} N_{\Delta} &= N'_{\Delta} e^{-(\Gamma_{\Delta} + k_{\text{pd}} + k_{\Delta})t} \\ N_{\Sigma} &= (N'_{\Sigma} + N'_{\Delta} f) e^{-k_{\Sigma}t} - N'_{\Delta} f e^{-(\Gamma_{\Delta} + k_{\text{pd}} + k_{\Delta})t}, \end{aligned} \quad (\text{A3})$$

where

$$f = 1 + \frac{k_{\text{pd}} + k_{\Delta} - k_{\Sigma}}{\Gamma_{\Delta}}. \quad (\text{A4})$$

With  $P(t) = k_{\text{pd}} N_{\Delta}$  and  $S(t) = k_{\Sigma} N_{\Sigma} + k_{\Delta} N_{\Delta}$ , we get

$$\frac{P(t)}{S(t)} = \frac{k_{\text{pd}}}{k_{\Sigma} \left[ \frac{N'_{\Sigma}}{N'_{\Delta}} + f \right] e^{(\Gamma_{\Delta} + k_{\text{pd}} + k_{\Delta} - k_{\Sigma})t} + k_{\Delta} - k_{\Sigma} f}. \quad (\text{A5})$$

Assuming  $k_{\text{pd}} = 0$  and  $k_{\Sigma} = k_{\Delta} = k$ , Eq. (A5) reduces to

$$\frac{P(t)}{S(t)} = \frac{k_{\text{pd}}}{k \left( \frac{N'_{\Sigma}}{N'_{\Delta}} + 1 \right)} e^{-\Gamma_{\Delta}t}, \quad (\text{A6})$$

establishing Eq. (4).

## APPENDIX B: LIFETIME OF THE ION BEAM

The ion beam lifetime is measured using photodetachment with the OPO at a photon energy of 1.240 eV (1000 nm). This

TABLE I. Estimated shift in the lifetime of the  $a^1\Delta$  state for  $k_{\Delta}/k_{\Sigma} = 2$ .

$1/k_{\Sigma}$ (s)	$1/\Gamma_{\Delta}$ (s)	$1/\Gamma_{\Delta} - 1/\Gamma$ (s)
250	15.39	0.89
300	15.24	0.74
350	15.13	0.63

photon energy is higher than the electron affinity of CH. Thus, photodetachment from all states of  $\text{CH}^-$  is possible, and the total lifetime of the ion beam is probed. The ion beam is stored for 1000 s, and the measurement is analogous to those in the upper panel of Fig. 3. In Fig. 5,  $P(t)$  is shown. The observed decay is not completely exponential, which is likely due to a combination of losses due to the space charge of the ion beam, and the decay of the  $a^1\Delta$  state. To obtain  $k_{\Sigma}$ , the data are fitted to an exponential function. Only a subset of the data is used in order to make sure there is no contribution from the  $a^1\Delta$  state. The fit in Fig. 5 is only including data recorded after 200 s of storage; at this point in time the  $a^1\Delta$  state has decayed completely. The choice of cutoff time affects the value of the fit, and accounting for this effect we estimate a beam lifetime of  $300 \pm 50$  s, corresponding to  $k_{\Sigma} \approx 3.3 \times 10^{-3}$ .

## APPENDIX C: INVESTIGATION OF $k_{\Delta} \neq k_{\Sigma}$

Equation (A5) is close to an exponential function with an effective decay rate  $\Gamma = \Gamma_{\Delta} + k_{\text{pd}} + k_{\Delta} - k_{\Sigma}$ . Some deviation from an exponential function may occur at small  $t$  when the terms  $k_{\Delta} - k_{\Sigma}f$  are comparable to the term with the exponential factor in the denominator. On the 100-s timescale of the experiment, however, an exponential is a valid approximation. In the analysis we perform a fit of an exponential function, and extract  $\Gamma = 14.5 \pm 0.2$  s. The decay rate of the  $a^1\Delta$  state is then  $\Gamma_{\Delta} = \Gamma - k_{\text{pd}} - k_{\Delta} + k_{\Sigma}$ . To investigate the effect of  $k_{\Sigma} \neq k_{\Delta}$ , we study  $\Gamma_{\Delta}$  as a function of  $k_{\Delta}/k_{\Sigma}$ . As discussed in the main text, here we assume  $k_{\text{pd}} = 0$  s $^{-1}$ . We constrain the discussion here to  $k_{\Delta}/k_{\Sigma} \geq 1$ , since it is unlikely that an electronically excited state has a lower cross section for collisional electron detachment than the ground state. Table I shows how  $\Gamma_{\Delta}$  is affected when  $k_{\Delta}/k_{\Sigma} = 2$ , also accounting for the uncertainty in  $k_{\Sigma}$ . We include this shift in our result by taking the largest deviation in Table I. To cover the full range of  $k_{\Delta}/k_{\Sigma}$  between 1 and 2, we set the shift to  $0.45 \pm 0.45$  s. We add this to our measured  $\Gamma$  and obtain  $14.9 \pm 0.5$  s for the final result.

- [1] T. J. Millar, C. Walsh, and T. A. Field, Negative ions in space, *Chem. Rev.* **117**, 1765 (2017).
- [2] N. Sakai, T. Sakai, Y. Osamura, and S. Yamamoto, Detection of  $\text{C}_6\text{H}^-$  toward the low-mass protostar IRAS 04368+2557 in L1527, *Astrophys. J.* **667**, L65 (2007).
- [3] V. Vuitton, P. Lavvas, R. Yelle, M. Galand, A. Wellbrock, G. Lewis, A. Coates, and J.-E. Wahlund, Negative ion chemistry in Titan's upper atmosphere, *Planet. Space Sci.* **57**, 1558 (2009).

- [4] E. Yurtsever, M. Satta, R. Wester, and F. A. Gianturco, On the formation of interstellar  $\text{CH}^-$  anions: Exploring mechanism and rates for  $\text{CH}_2$  reacting with  $\text{H}^-$ , *J. Phys. Chem. A* **124**, 5098 (2020).
- [5] D. Feldmann, Photoablösung von Elektronen bei einigen stabilen negativen Ionen, *Z. Naturforsch. A* **25**, 621 (1970).
- [6] A. Kasdan, E. Herbst, and W. Lineberger, Laser photoelectron spectrometry of  $\text{CH}^-$ , *Chem. Phys. Lett.* **31**, 78 (1975).

- [7] D. J. Goebbert, Photoelectron imaging of  $\text{CH}^-$ , *Chem. Phys. Lett.* **551**, 19 (2012).
- [8] D. Feller, Application of a convergent, composite coupled cluster approach to bound state, adiabatic electron affinities in atoms and small molecules, *J. Chem. Phys.* **144**, 014105 (2016).
- [9] M. Okumura, L. I. Yeh, D. Normand, and Y. T. Lee, The lifetimes for spontaneous emission from the  $X^3\Sigma^-(v=1)$  and  $a^1\Delta$  states of  $\text{CH}^-$ , *J. Chem. Phys.* **85**, 1971 (1986).
- [10] B. H. Lengsfeld, J. O. Jensen, and D. R. Yarkony, On the evaluation of lifetimes for spin-forbidden radiative transitions originating in coupling to states embedded in a continuum. application to  $\text{CH}^-$ , *J. Chem. Phys.* **88**, 3853 (1988).
- [11] S. Srivastava and N. Sathyamurthy, Radiative lifetimes of spin forbidden and spin allowed - transitions and complete basis set extrapolated ab initio potential energy curves for the ground and excited states of  $\text{CH}^-$ , *J. Chem. Phys.* **137**, 214314 (2012).
- [12] R. D. Thomas, H. T. Schmidt, G. Andler, M. Björkhage, M. Blom, L. Brännholm, E. Bäckström, H. Danared, S. Das, N. Haag, P. Halldén, F. Hellberg, A. I. S. Holm, H. A. B. Johansson, A. Källberg, G. Källersjö, M. Larsson, S. Leontein, L. Liljeby, P. Löfgren *et al.*, The double electrostatic ion ring experiment: A unique cryogenic electrostatic storage ring for merged ion-beams studies, *Rev. Sci. Instrum.* **82**, 065112 (2011).
- [13] H. T. Schmidt, R. D. Thomas, M. Gatchell, S. Rosén, P. Reinhed, P. Löfgren, L. Brännholm, M. Blom, M. Björkhage, E. Bäckström, J. D. Alexander, S. Leontein, D. Hanstorp, H. Zettergren, L. Liljeby, A. Källberg, A. Simonsson, F. Hellberg, S. Mannervik, M. Larsson *et al.*, First storage of ion beams in the double electrostatic ion-ring experiment: DESIREE, *Rev. Sci. Instrum.* **84**, 055115 (2013).
- [14] H. T. Schmidt, G. Eklund, K. C. Chartkunchand, E. K. Anderson, M. Kamińska, N. de Ruelle, R. D. Thomas, M. K. Kristiansson, M. Gatchell, P. Reinhed, S. Rosén, A. Simonsson, A. Källberg, P. Löfgren, S. Mannervik, H. Zettergren, and H. Cederquist, Rotationally Cold  $\text{OH}^-$  Ions in the Cryogenic Electrostatic Ion-Beam Storage Ring DESIREE, *Phys. Rev. Lett.* **119**, 073001 (2017).
- [15] E. Bäckström, D. Hanstorp, O. M. Hole, M. Kaminska, R. F. Nascimento, M. Blom, M. Björkhage, A. Källberg, P. Löfgren, P. Reinhed, S. Rosén, A. Simonsson, R. D. Thomas, S. Mannervik, H. T. Schmidt, and H. Cederquist, Storing keV Negative Ions for an Hour: The Lifetime of the Metastable  $^2P_{1/2}^o$  Level in  $^{32}\text{S}^-$ , *Phys. Rev. Lett.* **114**, 143003 (2015).
- [16] K. C. Chartkunchand, M. Kamińska, E. K. Anderson, M. K. Kristiansson, G. Eklund, O. M. Hole, R. F. Nascimento, M. Blom, M. Björkhage, A. Källberg, P. Löfgren, P. Reinhed, S. Rosén, A. Simonsson, R. D. Thomas, S. Mannervik, V. T. Davis, P. A. Neill, J. S. Thompson, D. Hanstorp *et al.*, Radiative lifetimes of the bound excited states of  $\text{Pt}^-$ , *Phys. Rev. A* **94**, 032501 (2016).
- [17] M. K. Kristiansson, S. Schiffmann, J. Grumer, J. Karls, N. de Ruelle, G. Eklund, V. Ideböhn, N. D. Gibson, T. Brage, H. Zettergren, D. Hanstorp, and H. T. Schmidt, Experimental and theoretical studies of excited states in  $\text{Ir}^-$ , *Phys. Rev. A* **103**, 062806 (2021).
- [18] S. Rosén, H. T. Schmidt, P. Reinhed, D. Fischer, R. D. Thomas, H. Cederquist, L. Liljeby, L. Bagge, S. Leontein, and M. Blom, Operating a triple stack microchannel plate-phosphor assembly for single particle counting in the 12-300 K temperature range, *Rev. Sci. Instrum.* **78**, 113301 (2007).
- [19] U. Mänz, A. Zilch, P. Rosmus, and H.-J. Werner, MCSCF-CI calculations of infrared transition probabilities in the  $\text{CH}^-$  and  $\text{NH}^-$  ions, *J. Chem. Phys.* **84**, 5037 (1986).
- [20] J. Fedor, K. Hansen, J. U. Andersen, and P. Hvelplund, Nonthermal Power Law Decay of Metal Dimer Anions, *Phys. Rev. Lett.* **94**, 113201 (2005).
- [21] E. K. Anderson, A. F. Schmidt-May, P. K. Najeeb, G. Eklund, K. C. Chartkunchand, S. Rosén, A. Larson, K. Hansen, H. Cederquist, H. Zettergren, and H. T. Schmidt, Spontaneous Electron Emission from Hot Silver Dimer Anions: Breakdown of the Born-Oppenheimer Approximation, *Phys. Rev. Lett.* **124**, 173001 (2020).
- [22] J. E. Sansonetti and W. C. Martin, Handbook of basic atomic spectroscopic data, *J. Phys. Chem. Ref. Data* **34**, 1559 (2005).
- [23] T. Carette and M. R. Godefroid, Theoretical study of the  $\text{C}^-$   $^4S_{3/2}^o$  and  $^2D_{3/2,5/2}^o$  bound states and C ground configuration: Fine and hyperfine structures, isotope shifts, and transition probabilities, *Phys. Rev. A* **83**, 062505 (2011).